Adiabatic Shear Failure and Dynamic Stored Energy of Cold Work

D. Rittel,* Z. G. Wang, and M. Merzer†

Faculty of Mechanical Engineering, Technion, 32000 Haifa, Israel

(Received 9 June 2005; published 22 February 2006)

Dynamic testing of statically predeformed specimens of magnesium (AM50) shows that the failure strain increases with the level of prestrain. Interrupted and other dynamic tests show that the temperature rise prior to localization has only a minor influence on adiabatic shear band (ASB) formation. For all the tests, the dynamic deformation energy until ASB formation is found to be relatively constant, indicating that ASB is dependent almost solely on dynamic deformation processes, with quasistatic and thermal effects prior to localization being very marginal. We suggest the concept of a constant dynamic mechanical energy (toughness) as a quantitative criterion for ASB formation—this concept being related physically to the dynamic stored energy of cold work. All in all, the tests indicate that ASB failure is more dependent on energy considerations that on strain criteria, as has been considered until now.

DOI: 10.1103/PhysRevLett.96.075502 PACS numbers: 62.20.Fe, 62.20.Mk

Adiabatic shear failure is a well-known failure mechanism that is uniquely experienced in dynamic loading situations [1,2]. The homogeneous deformation tends to localize into a narrow band followed by catastrophic failure. Because of the typical short time scales involved, the phenomenon is considered to be adiabatic with large temperature increases, especially inside the band. Many materials fail by adiabatic shear banding (subsequently referred to as ASB) in an uncontrolled manner. A vast body of literature has been dedicated to the material aspects of adiabatic shear failure [1,2]. A basic criterion has been proposed by Zener and Hollomon [3], which states that ASB is governed by the competition between strain hardening and thermal softening of the material, so that the critical conditions for ASB formation are met when the material looses its strain-hardening capacity. This criterion has been the basic ingredient for the vast majority of subsequently proposed criteria. These criteria were developed for specific constitutive models, and it can be noted that they all point to a critical strain value for the onset of the unstable failure process [2,4]. By contrast with the ample literature dedicated to the material aspects of ASB's, there are very few experimental attempts to investigate the mechanical aspects of the problem. Noticeable exceptions are the work of Marchand and Duffy [5] on dynamic torsion with simultaneous temperature measurements, and also work by Johnson and Cook [6] who verified the validity of their constitutive model for the prediction of the critical strain to failure. Other experimental investigations were aimed at provoking controlled shear band nucleation from a crack tip, as in Zhou *et al.* [7,8], and in this context, the concept of shear band toughness was invoked.

The purpose of the present work is to bring new experimental evidence on adiabatic shear banding from a mechanical point of view, emphasizing the effects of the prior mechanical history of the material (prestrain) and thermomechanical aspects of the localization process.

The selected material is a magnesium-aluminum alloy (AM50), with a typical grain size of 10 μm, supplied as 12 mm diameter rods [9]. Specimens were tested in the as-received condition. Quasistatic tests were performed on a servo-hydraulic testing machine (MTS 810), while high strain-rate tests were performed on a 19 mm diameter split Hopkinson pressure bar [10]. Two specimen geometries were tested: cylinders and shear compression specimens (SCS). Both gave identical stress-strain curves indicating that our findings are not specimen-geometry dependent. [The SCS is a cylinder with a pair of diametrically opposed 45° grooves. It has been especially developed and validated both numerically [11,12] and experimentally [13–15]. One of its advantages is the well-defined (pressure) dominant shear deformation of its gauge section.]

Figure 1 presents typical stress-strain curves obtained at various strain rates. It shows that AM50 is moderately strain-rate sensitive, with its mechanical properties being only slightly dependent on the strain rate in the dynamic regime ($\dot{\varepsilon} \approx 10^3\ \mathrm{s}^{-1}$). AM50 has a strong strain-hardening capacity until failure, in both quasistatic and dynamic deformation regimes. The typical static failure strain is $\varepsilon_{\mathrm{FS}} \approx 0.14$, while for dynamic failure it is slightly higher, $\varepsilon_{\mathrm{FD}} \approx 0.17$. For dynamically compressed cylinders, the typical failure mode includes the formation of two conical fragments, as opposed to barreling, with a 45° apex, as shown in Fig. 1 (insert). The envelope of the cones is formed by adiabatic shear banding. The SCS specimens also fail by adiabatic shear at high strain rates. In all cases, the dynamic final failure stage is quite abrupt. Thus, once a shear band has nucleated, it propagates and fractures very rapidly. This well-defined initiation stage makes AM50 an ideal model material for ASB studies.

Two sets of experiments were performed: ''static dynamic'' and ''dynamic dynamic.'' The ''static-dynamic'' tests, performed on SCS specimens, started with static preloading to a predetermined strain, $\varepsilon_{\mathrm{prestrain}}$, followed

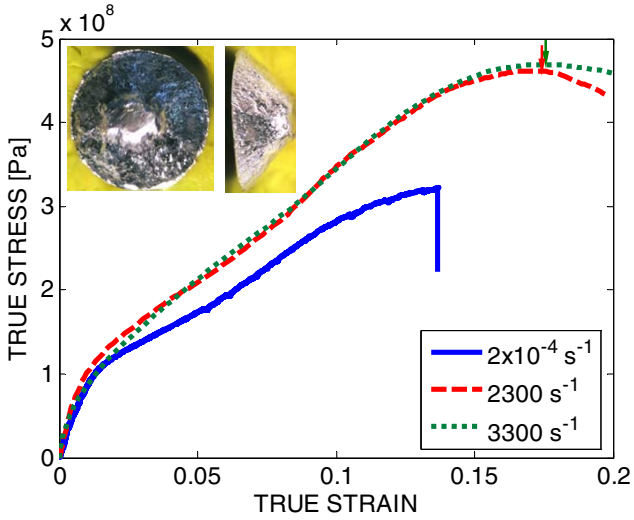

FIG. 1 (color online). Typical quasistatic and dynamic stress-strain characteristics of AM50 alloy. Note the large strain-hardening capacity of the material and its relative lack of strain-rate sensitivity in the dynamic regime. The maximum dynamic failure strain is indicated by an arrow. The insert shows the typical dynamic failure mode of a cylindrical specimen. Two conical fragments are generated, whose envelope is caused by adiabatic shear.

by dynamic loading. Figure 2(a) shows that the total strain (static and dynamic) to failure ε_{tot} increases noticeably with the level of prestrain. This is contrary to the constant failure strain criterion requiring failure strain to remain constant. The total strain may reach $\varepsilon_{\text{tot}} \approx 0.22$ and is larger than the characteristic failure strains obtained from pure quasistatic and dynamic tests $-\varepsilon_{\text{FS}} \approx 0.14$, $\varepsilon_{\text{FD}} \approx 0.17$, respectively. An additional quantitative insight is gained by calculating the dynamic mechanical energy involved until failure, i.e., the area of the dynamic stress-strain curve up to instability (indicated by the arrows in Figs. 1 and 2). The result (Fig. 3) shows that the dynamic mechanical energy is practically constant, irrespective of the initial prestrain levels, which can reach very large values ($\varepsilon_{\text{prestrain}} \approx 0.12 = 0.85\varepsilon_{\text{FS}}$). And, even at these large prestrain levels, the drop in mechanical energy still remains quite small.

Similar ''static-dynamic'' tests were also carried out on a tungsten base heavy alloy (WHA) [14], and a Ti6Al4V alloy. Large prestrain levels were applied, (up to $\sim 0.5\varepsilon_{\text{FS}}$). For both materials, the dynamic deformation energy was again observed to be constant irrespective of the level of prestrain, thus validating and extending the observations done for AM50. (Detailed results are to be reported elsewhere.)

The ''dynamic-dynamic'' tests are interrupted dynamic tests on cylindrical specimens. These specimens were dynamically loaded to a predefined strain level, using a stop-ring technique which limits the displacement of the incident Hopkinson bar. After a pause of 15 min or more,

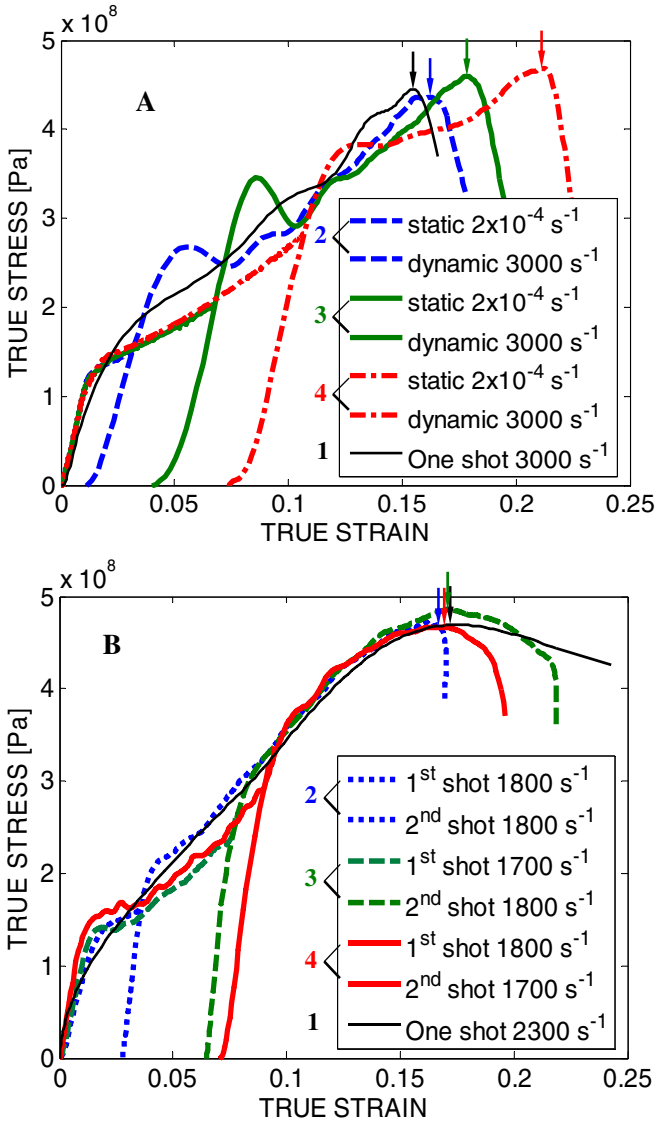

FIG. 2 (color online). Typical stress-strain characteristics of AM50 alloy. (a) Quasistatic preload tests followed by dynamic tests. Note that the maximum strain (arrow) increases steadily with the level of prestrain. The thin solid curve shows a stress-strain curve for a monotonic dynamic test at a similar strain rate. (b) Interrupted dynamic tests. The thin solid curve shows a stress-strain curve for a monotonic dynamic test at a similar strain rate. All the curves have almost constant maximum strains.

they were reloaded dynamically. Figure 2(b) shows the composite stress-strain curve from these tests, together with a monotonic (single shot) stress-strain curve for comparison. The results clearly show that various interruptions did not affect the overall dynamic response of this material, and, in particular, the final failure strain.

This is of particular significance when thermal aspects are considered. The 15 min-plus interval between the two stages of the dynamic tests effectively cooled down any temperature rise from the first stage and created room temperature conditions at the start of the second stage.

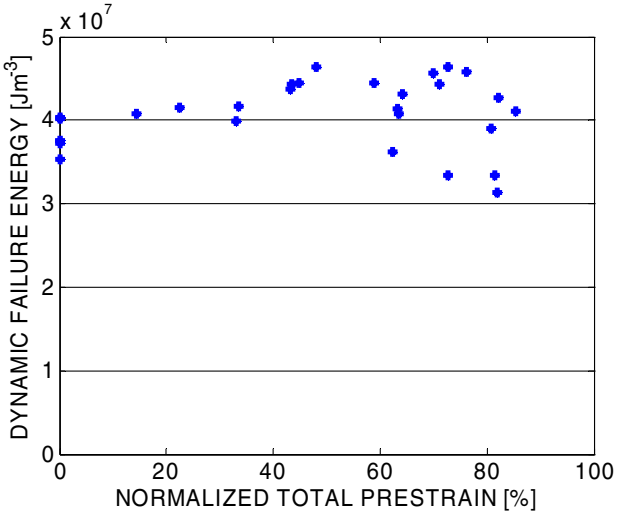

FIG. 3 (color online). Plot of the dynamic mechanical energy of AM50 as a function of the normalized prestrain $\frac{\varepsilon_{\text{prestrain}}}{\varepsilon_{\text{FS}}} \times 100$. Note that the energy is remarkably constant up to normalized prestrain levels of the order of 0.7, beyond which it decreases slightly. The overall influence of the quasistatic prestrain on the dynamic mechanical energy is minor.

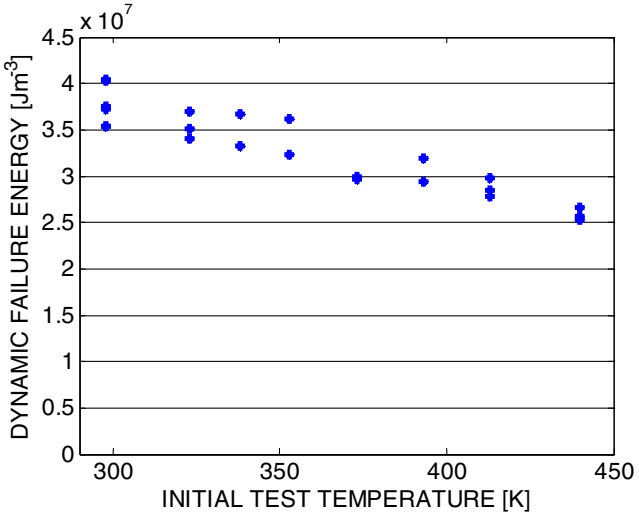

FIG. 4 (color online). Plot of the dynamic mechanical energy of AM50 as a function of the initial test temperature. Note that the calculated maximum homogeneous temperature rise is $T_{\max} = 336$ K, at which the energy is almost not affected.

The temperature at final failure was then solely due to the heat generated in the second stage alone. This heat is different for each second stage curve in Fig. 2(b), and thus the temperature at failure is also different. Such a difference would imply different failure strains, but this is not the case—all the failure strains are practically the same. This indicates that thermal effects have only a minor influence on ASB formation.

This issue was further investigated by means of a series of dynamic tests carried out at various initial temperatures, up to 433 K. Figure 4 shows that the dynamic mechanical energy decreases only slightly at the higher test temperatures, indicating that thermal softening is of marginal importance.

The results presented here show that the widely accepted concept of a critical strain cannot strictly predict the onset of adiabatic shear failure, if the overall mechanical history of the material is to be taken into account. We propose an alternative criterion to identify the onset of ASB, using the value of the overall dynamic mechanical energy up to catastrophic failure, at which it reaches a critical value (toughness). This value was measured for different materials, the (relatively) rate-insensitive AM50, and the rate-sensitive WHA and Ti6Al4V alloys. For various large static prestrain levels, the mechanical energy is remarkably constant both for AM50, and for WHA and Ti6Al4V alloys. One could therefore postulate that this critical mechanical energy is a material property (toughness) which can easily be measured and implemented in a numerical procedure. Being a scalar, the mechanical energy also has the practical advantage of overcoming the issue of multiaxial strain situations for which each strain component, or an equivalent strain, must be considered separately.

Further evidence for the insignificance of thermal effects prior to localization can be found in two points:

(1) It has long been established that the mechanical energy splits partly into stored energy of cold work [16] and into thermal energy, as shown in the early work of Taylor and Quinney [17]. A rapid estimation of the temperature rise prior to shear localization can be made, assuming the limiting case in which all of the mechanical energy goes into heat. In this case,

$$\beta \int_0^{\varepsilon_{\text{FD}}} \sigma_{ij} de_{ij}^p = \rho C_p \Delta T, \tag{1}$$

where σ and e^p are the stress and plastic strain tensors, ρ is the material density, C_p is the heat capacity, and ΔT is the temperature rise. The factor β expresses the variable ratio of the thermal to mechanical energy, whose maximum value can be taken as (1). Inserting typical (average) values $\sigma = 400$ MPa, $e^p = 0.17$, $\rho = 1740$ kg/m^3, and $C_p = 1023$ J/kg K, one obtains a temperature rise of $\Delta T = 38$ K at most. For an incipient melting temperature of AM50 of $T_M = 708$ K, the present temperature rise (starting at room temperature, 298 K) means that the gauge section has reached about $T_{\max} = 0.48 T_M$ prior to localization. Such a temperature is not negligible and the material is expected to undergo thermal softening. However, in the dynamic-dynamic tests, the material was not allowed to experience such a continuous temperature rise, and it nevertheless showed adiabatic failure characteristics of a similar nature to those observed in monotonic dynamic tests.

(2) The high temperature tests (Fig. 4) were performed up to a homologous temperature of $T_{\text{hom}} = 0.6$ (actual $T = 433$ K) that is far higher than any temperature reached during the homogeneous stage of the dynamic deformation ($T_{\max} = 336$ K). Yet, the dynamic mechanical energy remained relatively unaffected at $T_{\max}$.

All these observations suggest that the specimen's temperature prior to adiabatic shear localization has only a very minor effect on the onset of ASB formation, in agreement with results of Clos *et al.* [18] who report a minor temperature rise prior to localization in their steel specimens. From a practical point of view, thermal effects can be verified experimentally through real time monitoring of the specimen's temperature. The onset of the localization process can be identified as the point where the measured temperature rise exceeds that which is calculated assuming a total conversion of mechanical energy into heat [$\beta = 1$ in Eq. (1)].

The fact that ASB formation is apparently totally dependent on the dynamic stored energy of cold work suggests that relevant physical mechanisms are most likely related to the specific microstructure (e.g., dislocation patterns and hardening) that results from dynamic loading only, in agreement with the observations of Kennedy and Murr [19].

To summarize, until now, the onset of adiabatic shear band (ASB) failure has been considered to be dependent mainly on strain considerations with energy factors being considered minor. Our work suggests the opposite. Energy factors are the main criterion for the onset of ASB failure, while the critical strain criterion applies in more restricted conditions.

In addition, this study shows the following specific points. The dynamic stored energy of cold work is experimentally identified as the governing factor for ASB formation. This is because: (a) the dynamic mechanical energy has a constant value (toughness) at the onset of ASB formation, for a large range of quasistatic prestrain levels and initial test temperatures. (b) The homogeneous specimen temperature (either adiabatic rise or from test conditions) prior to strain localization has a very minor influence on the subsequent ASB formation, emphasizing the importance of cold work independent of thermal heating.

This constant energy of cold work reflects a state beyond which the material's microstructure can no longer be modified, so that all the mechanical energy goes to heat. As such, this point can be identified experimentally.

The results presented here appear to be of a general character since identical results have also been obtained for annealed Ti6AL4V and tungsten base (WHA) heavy alloys.

The support of the Israel Science Foundation (Grant No. 2002968) is gratefully acknowledged.

*Corresponding author.
Email address: merittel@technion.ac.il
†On sabbatical leave from RAFAEL, POB 2250 Haifa, 31021 Israel.

[1] M. A. Meyers, *Dynamic Behavior of Materials* (Wiley, New York, 1994).
[2] Y. L. Bai and B. Dodd, *Adiabatic Shear Localization-Occurrence, Theories and Applications* (Pergamon, New York, 1992).
[3] C. Zener and J. H. Hollomon, J. Appl. Phys. **15**, 22 (1944).
[4] S. E. Schoenfeld and T. W. Wright, Int. J. Solids Struct. **40**, 3021 (2003).
[5] A. Marchand and J. Duffy, J. Mech. Phys. Solids **36**, 251 (1988).
[6] G. R. Johnson and W. H. Cook, *Proceedings of the 7th International Symposium on Ballistics, The Hague, The Netherlands* (American Defense Preparedness Association, The Netherlands, 1983).
[7] M. Zhou, A. J. Rosakis, and G. Ravichandran, J. Mech. Phys. Solids **44**, 981 (1996).
[8] M. Zhou, A. J. Rosakis, and G. Ravichandran, J. Mech. Phys. Solids **44**, 1007 (1996).
[9] The AM50 (ASTM B94) rods used in this study were manufactured by Dead Sea Magnesium Ltd. The main component is Mg, with the following alloying elements (in weight %): Al: 4.5–5.3, Mn: 0.28–0.5, Zn: 0.2, Si: 0.05, Cu: 0.008, Ni: 0.001, and Fe: 0.004. Microstructural characterization, using transmission electron microscopy (TEM) and energy dispersive x-ray analysis (EDX), reveals an Al-Mg solid solution (matrix) which contains elongated (typically 1 μm long) β phase ($Mg_{17}Al_{12}$) and Al_8Mn_5 precipitates.
[10] H. Kolsky, Proc. R. Soc. B **62**, 676 (1949).
[11] A. Dorogoy and D. Rittel, Exp. Mech. **45**, 167 (2005).
[12] A. Dorogoy and D. Rittel, Exp. Mech. **45**, 178 (2005).
[13] D. Rittel, S. Lee, and G. Ravichandran, Exp. Mech. **42**, 58 (2002).
[14] D. Rittel, R. Levin, and A. Dorogoy, Metall. Mater. Trans. A **35**, 3787 (2004).
[15] M. Vural, D. Rittel, and G. Ravichandran, Metall. Mater. Trans. A **34**, 2873 (2003).
[16] M. B. Bever, D. L. Holt, and A. L. Titchener, Prog. Mater. Sci. **17**, 5 (1973).
[17] G. I. Taylor and H. Quinney, Proc. R. Soc. A **143**, 307 (1934).
[18] R. Clos, U. Schreppel, and P. Veit, J. Phys. IV (France) **110**, 111 (2003).
[19] C. Kennedy and L. E. Murr, Mater. Sci. Eng. A **325**, 131 (2002).